JOM, Vol. 70, No. 6, 2018
https://doi.org/10.1007/s11837-018-2810-7

Graphene-Reinforced Aluminum Matrix Composites: A Review of Synthesis Methods and Properties

FEI CHEN,[1] NIKHIL GUPTA,[1] RAKESH K. BEHERA,[1,3] and PRADEEP K. ROHATGI[2]

1.—Composite Materials and Mechanics Laboratory, Mechanical and Aerospace Engineering Department, New York University, Tandon School of Engineering, 6 MetroTech Center, Brooklyn, NY 11201, USA. 2.—Materials Science and Engineering Department, CEAS, University of Wisconsin-Milwaukee, 3200 N. Cramer Street, Milwaukee, WI 53211, USA. 3.—e-mail: rakesh.behera@nyu.edu

Graphene-reinforced aluminum (Gr-Al) matrix nanocomposites (NCs) have attracted strong interest from both research and industry in high-performance weight-sensitive applications. Due to the vastly different bonding characteristics of the Al matrix (metallic) and graphene (in-plane covalent + inter-plane van der Waals), the graphene phase has a general tendency to agglomerate and phase separate in the metal matrix, which is detrimental for the mechanical and chemical properties of the composite. Thus, synthesis of Gr-Al NCs is extremely challenging. This review summarizes the different methods available to synthesize Gr-Al NCs and the resulting properties achieved in these NCs. Understanding the effect of processing parameters on the realized properties opens up the possibility of tailoring the synthesis methods to achieve the desired properties for a given application.

INTRODUCTION

Aluminum (Al), one of the most widely used nonferrous metals, has physical and mechanical properties (Fig. 1a, b and Table I)[1] that are of interest to many structural applications. High specific strength, low coefficient of thermal expansion, high corrosion resistance and low density are some of the key properties that enable applications of Al and its alloys in the transportation, defense, construction, energy distribution and consumer goods industries. However, Al alloys suffer from poor tribologic properties, and improving the wear response as well as mechanical properties by using a variety of reinforcements including ceramics such as Al_2O_3, SiC, BN and B_4C is a major focus.[2] Nanoscale reinforcements with carbon nanotubes and graphene have allowed developing composites that not only have the desired mechanical properties, but also functional properties such as self-lubricating surfaces.[3,4] In particular, graphene has shown tremendous potential to improve the mechanical, electrical, thermal and tribologic properties of the composite compared with the unreinforced alloys.[3,5] The present review is focused on discussing the synthesis methods and properties of graphene-reinforced aluminum (Gr-Al) matrix nanocomposites (NCs). Graphene is now available in industrial quantities, and it is possible to make large-scale components of graphene-reinforced composites.[6]

Graphene

Graphene, a flat monolayer of carbon atoms packed into a two-dimensional form (Fig. 1c and d), has attracted attention because of its high strength, high modulus, excellent electrical, thermal and optical properties, and extremely high specific surface area available for novel chemistry (Table I).[7] Due to the unique combination of properties, graphene is used in a wide range of applications such as chemical sensors, energy storage, transistors, portable electronics and components in the automotive and aviation industries.[8] To take advantage of the multifunctional properties of graphene, researchers have attempted to synthesize high-quality graphene at the industrial scale to satisfy the current demand. A simple but effective "scotch tape" or "mechanical exfoliation" method first demonstrated that graphene can be exfoliated

(Published online March 16, 2018)

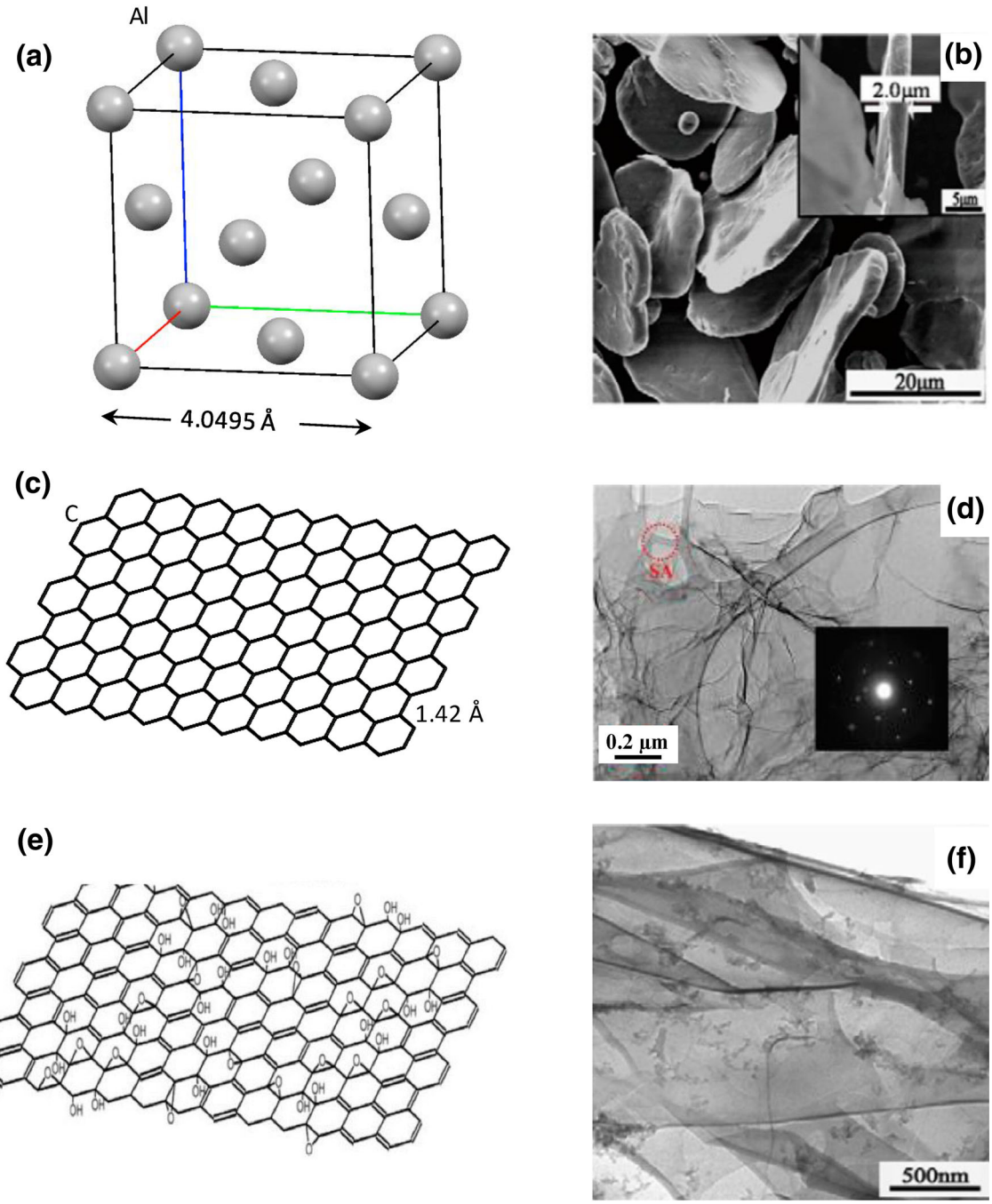

Fig. 1. (a) Face-centered cubic structure of aluminum (lattice parameter 4.0495 Å). (b) SEM image of flaky Al powder with average flake thickness shown in the inset.[30] (c) Structural arrangement of a single layer of defect-free graphene with C–C distance of 1.42 Å. (d) Transmission electron micrograph (TEM) of graphene platelet showing wrinkled morphology (inset shows the selected area diffraction of hexagonal graphene cell).[31] (e) Structural representation of graphene oxide (GO) showing the presence of functional groups compared with pure graphene.[3] (f) TEM image of GO nanosheets.[30].

into mono-layers from bulk graphite using adhesive tapes.[9–11] Other synthesis methods developed to create single- or a-few-layer graphene in small quantities include growth from a solid carbon source, sonication, cutting open carbon nanotubes, carbon dioxide reduction and graphite oxide reduction.[12–16] However, further work is necessary to synthesize high-quality graphene using some of these methods. Chemical vapor deposition (CVD) is commonly used for industrial-scale production of graphene.[13,17–19] With the fracture strength and Young's modulus reported as high as 130 GPa and 1

Table I. List of various properties of aluminum and graphene

Properties	Aluminum[1] *	Single layer of graphene[7]
Tensile strength	40–700 MPa	130 GPa
Young's modulus	70 GPa	0.5–1 TPa
Thermal conductivity	237 W m^{-1} K^{-1}	4840–5300 W m^{-1} K^{-1}
Coefficient of thermal expansion	21–24 × 10^{-6}/K	− 6 × 10^{-6}/K
Electron mobility (at 298 K)	12 cm^2 V^{-1} s^{-1}	15,000 cm^2 V^{-1} s^{-1}
Transmittance		> 95% for 2-nm-thick film > 70% for 10-nm-thick film
Theoretical specific surface area		2630 m^2 g^{-1}

*Data extracted from ASM Handbook Volume 2.

TPa, respectively, graphene is arguably the strongest and stiffest material available and is considered ideal as a reinforcement for both polymer and metal matrix composites.

Graphene/Metal Nanocomposites

Graphene-reinforced composites, especially polymer matrix nanocomposites (PMNCs), are extensively studied in the literature.[20–22] However, challenges to synthesize have limited the progress in graphene-reinforced metal matrix nanocomposites (MMNCs). One of the key issues is the widely different bonding characteristics of graphene and aluminum (metallic bonding in matrix and covalent + van der Waals bonding in the graphene). The strong interplanar van der Waals interaction between graphene sheets in a metallic environment promotes agglomeration in the form of a separate graphene phase, which is detrimental for the MMNC properties. Therefore, significant effort has been invested in developing novel synthesis methods to achieve uniform distribution and improved bonding of graphene with the matrix alloy.[16,23–25] Various methods such as (1) ball milling to mechanically exfoliate graphene in the matrix,[26,27] (2) CVD for layer-by-layer deposition of graphene and metal[13,19] and (3) flake powder metallurgy[23,28–30] have been examined to avoid agglomeration of graphene in the metal matrix.

To take advantage of the matured synthesis techniques, hydrophilic graphene oxide (GO) (Fig. 1e and f)[3,30] is used as the starting material for most of the graphene-reinforced MMNCs. Graphene is obtained by either chemical or thermal reduction of GO during the synthesis of the MMNCs. The synthesis methods and properties of graphene reinforced NCs are discussed in the following sections.

SYNTHESIS AND PROPERTIES

Table II lists the chronologic development of synthesis strategies attempted for Gr-Al NCs.[4,15,16,23,25,26,28,30–43] One of the first reported efforts, by Bartolucci et al., to synthesize Gr-Al NCs used a combination of ball milling, hot isostatic pressing (HIP) and the extrusion process to synthesize the MMNCs.[31] Graphene was obtained through the oxidation followed by exfoliation route. First, graphite was oxidized in a solution of sulfuric acid, nitric acid and potassium chlorate for 4 days. The graphite oxide powder then underwent thermal exfoliation at ~ 1050°C in argon atmosphere to remove a large portion of the oxygen to achieve ~ 3–4 carbon sheets thick graphene platelets (Fig. 1d). To produce the Gr-Al composite, pure aluminum powder (average particle size of 22 μm) was first mixed with graphene by blending in an acoustic mixer for 5 min and then milled for an hour in argon atmosphere. The resulting mixture was consolidated via HIP performed at an average temperature of 375°C for 20 min and then extruded with a 4:1 ratio. The mechanical properties of the Gr-Al NC synthesized using this route were surprisingly inferior to pure Al. The Gr-Al NC showed a 12.5% reduction in Vickers hardness, 18% reduction in tensile strength, 34% reduction in yield strength and 50% reduction in ductility compared with that of pure Al used as the matrix. While the reduction in ductility is in agreement with the behavior of other MMNCs, the deterioration of strength and hardness values needed further explanation. A closer examination of the microstructure (Fig. 2) revealed formation of a brittle aluminum carbide (Al_4C_3) phase, which is attributed to the large number of defects or reaction sites (exposed prism planes) in graphene due to thermal exfoliation.[12,44] While the mechanical properties of the polymer matrix composites are reported to improve because of defects in graphene, this is measured to be exactly opposite for the Al matrix.[45,46] Figure 2 also includes results for 1 wt.% multi-walled carbon nanotubes (MWNT)-Al NCs, which are observed to have higher mechanical properties than pure Al. Therefore, this study established that processing is key to improving the mechanical properties of Gr-Al NCs, and care must be taken to avoid the formation of undesired phases during synthesis.

Following the work of Jiang et al.[47] in synthesizing CNT-Al NCs using flake powder metallurgy (PM), Wang et al.[30] used the novel flake PM

Table II. Chronologic development in the synthesis of graphene-reinforced aluminum metal matrix composites. All the main results show comparison with corresponding unreinforced Al unless specifically mentioned

References	Reinforcement	Synthesis method	Main results
Year 2011			
31	Al-0.1 wt.% graphene	Ball milling, hot isostatic pressing, hot extrusion	Decrease in hardness Tensile strength (18% decrease) Yield strength (34% decrease) Reduced ductility
16	Al-0.3 wt.% graphene nanoflakes (GNFs)	Ball milling, hot isostatic pressing, extrusion	Tensile strength (25% increase) Yield strength (58% increase)
25	Al-3 wt.% graphene nanoplatelets (GNPs)	Ultrasonication, cold pressing, sintering	Hardness (max ~ 66% increase) Compressive strength (max ~ 21% increase)
Year 2012			
30	Al (surface modified)- 0.3 wt.% graphene nanosheets (GNSs)	Powder metallurgy, compacting and consolidation, hot extrusion	Tensile strength (62% increase) Ductility (~50% reduction in strain)
32	Al-5 wt.% GNPs	Mixing, cold pressing, sintering (600°C)	Hardness (~ 35% increase) Compressive strength (~ 21% increase)
33	Al2124-3 wt.% graphene	Ball milling, cold pressing, hot extrusion	Hardness (47.5% increase)
Year 2014			
26	Al6061-1 wt.% graphene	Ball milling, pre-compaction and hot compaction	Flexural strength (increased by 47% for 60-min and 34% for 90-min)[a]
35	Al-0.25, 0.50, 1.0 wt.% graphene nanoplatelets (GNPs)	Ball milling, cold consolidation and sintering	Hardness (max increase of 1.325 times occurs for 2-h sintering time and 5-h milling at 1.0 wt.%)[b]
23	Al-0.3 wt.% reduced graphene oxide (RGO)	Stirring, thermal reduction, hot pressing	Hardness (17% increase) Modulus (18% increase)[c]
34	Al5052-H32-graphene oxide/ water colloid (15 mg ml^{-1})	Friction stir processing (FSP)	Tensile strength (~ 12% decrease) Ductility (50.5% increase) Thermal conductivity (16% increase)
28	(Al-3.9 Cu-1.5 Mg) - 0.5 wt.% GNFs	Wet ball milling, hot isostatic pressing, hot extrusion	Tensile strength (25% increase) Yield strength (50% increase)
36	Al-0.3 wt.% GNPs	Stirring, sintering, hot extrusion	Hardness (12% increase) Tensile strength (11% increase) Yield strength (15% increase) Compressive strength (7% decrease) Compressive yield strength (unchanged) Ductility (29% decrease)
Year 2015			
37	Al-0.5, 1, 1.5, 2 wt.% GNFs	Blending, cryomilling, degassing and hot extrusion	Tensile strength (18% increase for 0.5wt.%, 69% increase for 1.0wt.%); yield Strength (8.8% increase for 0.5wt.% and 55% increase for 1.0wt.%)[d] Ductility generally decreased
38	Al-0.7 wt.% few-layer graphene (FLG)	Ball milling, hot rolling	Yield strength (70% increase) Ductility (~ 86% decrease)
43	Al-0.05 wt.% graphene	Ball milling, high-pressure torsion (HPT)	Hardness (67% increase with respect to HPT Al)[e]
Year 2016			
39	Al2024–0.5 vol.% FLG	Ball milling, hot pressing, sintering	Yield strength (2 times higher)[f]

Table II. continued

References	Reinforcement	Synthesis method	Main results
4	Al-1 wt.% GNPs	Wet ball milling, cold pressing, hot pressing	Hardness (7% decrease)
Year 2017			
41	Al6061-0.7 wt.% ultrafine Ni nanoparticle-decorated graphene hybrid	CVD, ball milling, hot pressing	Tensile strength (30% increase) Yield strength (75% increase)
15	Gas atomized (GA)/ mechanically milled (MM) Al-1 wt.% FLG/1 wt.% FLG oxide (FLGO)	Wet method, cold compaction, sintering	Hardness (max increase of 40% between MM-FLGO and MM Al) Compressive yield strength (max increase of 52% between GA-FLGO and GA Al)
42	Al6061-2 vol.% graphene	Mixing, spark plasma sintering	Constant hardness Decrease in modulus
40	Al-0.5 wt.% RGO	Ultrasonication, cold pressing, sintering	Increase in hardness

[a]30-min of milling was not enough for the graphene to be uniformly dispersed throughout the Al6061 matrix, so no enhancement.[b]2-h sintering shows no clusters of GNPs in SEM micrographs, which corroborates a homogeneous dispersion.[c]RGO sheets are uniformly dispersed in the Al matrix.[d]Till 1 wt.% GNFs then strengths decrease.[e]Hardness is similar with respect to ball-milled +HPT Al.[f]Compressive yield strength is three times higher than monolithic Al at 350°C.

approach to fabricate graphene nanosheet (GNS, comprising a few graphene layers)-Al NCs. The use of GNSs significantly improved the uniform dispersion of the carbonaceous material in the matrix. The flake PM method had a few major steps in preparing the GNS-Al composite with initial formation of GOs and Al flakes. Single- or a-few-layered GOs are exfoliated by ultrasonication of the GO in deionized water. It is important to point out that graphite oxide is a multilayered system, while GO contains a single or a few layers of graphene. Compared with pure graphene, GO contains four functional groups (hydroxyl, carbonyl, carboxylic and epoxy groups) on the surface (Fig. 1e). The presence of these functional groups not only expands the layer separation, but also makes it easier for the GOs to disperse in the matrix and form a more stable solution than graphene.[14] For the matrix material, spherical Al powders ($\sim$ 10 μm in diameter) were transformed into 2-μm-thick Al flakes by ball milling (Fig. 1b). The surface of the flakes is modified by polyvinyl alcohol (PVA) in this step for GO interaction. The PVA-modified flakes and GO are mechanically stirred to form the GO-Al composite powders. Figure 3a and b shows the scanning electron microscope (SEM) image comparison between an Al flake surface with and without GO nanosheets, respectively. The fine wrinkles in Fig. 3a indicate uniform distribution of GO nanosheets resulting from the shape compatibility of the two mixing constituents.[30] These composite powders were heated to 550°C under argon atmosphere to reduce the GO nanosheets to GNSs, resulting in the GNS-Al NC powders. Finally, compaction, sintering and hot extrusion at a ratio of 20:1 were applied to consolidate the powders into the bulk GNS/Al composite.

A comparison of the stress–strain response of pure Al and 0.3 wt.% GNS-Al NC confirmed a $\sim$ 62% enhancement in tensile strength (249 MPa) in the MMNC, while the ductility reduced by almost half (13% elongation) that of the pure Al sample (Fig. 3c). This study established that GNS positively reinforces the MMNC. While there is a $\sim$ 100 MPa increase in tensile strength compared with pure Al, theoretical predictions using the rule of mixture estimated the actual increase should be $\sim$ 500 MPa for 0.3 wt.% GNS-Al NCs. This significant difference can be addressed by the assumptions taken in the theoretical calculations to what is achieved during experimental synthesis. The theoretical calculations used 125 GPa[48] as the fracture strength of a perfectly aligned defect-free single layer of graphene along the loading direction, which is not the case experimentally. The GNSs synthesized experimentally had more than one layer of graphene, contributing to the reduction in strength. Also, the out-of-plane strength of graphene is well below the in-plane strength. Hence, any misalignment with respect to the loading direction leads to a reduction in the strength of the mixture. In addition, the interfacial interaction between the GNS and Al matrix is another factor that contributes to the variation in strength. Bartolucci et al.[31] showed that the formation of Al_4C_3 can adversely affect the strength of the composite. This analysis suggested that improved understanding of experimental parameters could enable realizing better mechanical properties of the

NC by focusing on uniform distribution of the graphene phase and its bonding with the Al matrix. Figure 3d also includes the SEM image of the fractured surface of the MMNC.

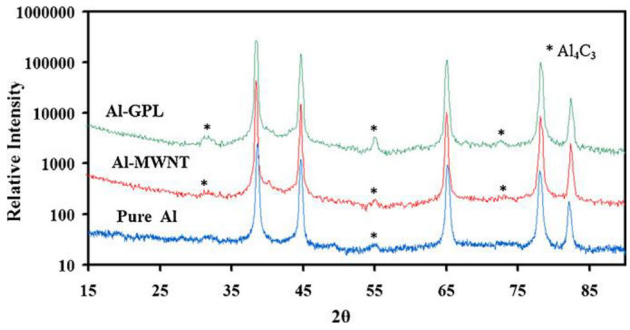

Fig. 2. X-ray diffraction of pure aluminum, Al–1.0 wt.% MWNT composite and Al–0.1 wt.% graphene composite after extrusion.[31]

To understand the effect of experimental parameters on the mechanical properties, Bastwros et al.[26] examined the impact of milling time on Gr-Al6061 NCs fabricated using the semi-solid processing technique. This technique has been shown to improve properties of CNT-Al NCs. In this method, monolayers or a-few-layer GOs were exfoliated with the aid of ultrasonication from expanded graphite (using Brodie's method[49]). The GOs and Al6061 alloy (average particle size of 13.8 μm) were mechanically alloyed using ball milling at ambient conditions. A pre-compaction step of the mixture was performed at 50 MPa at room temperature followed by hot compaction at 100 MPa in the semi-solid region of Al6061 (at 630°C with $\sim$ 18% liquid phase) to achieve the Gr-Al6061 NCs. Since properties of the composite depend on the dispersion of the reinforcement, Bastwros et al.[26] systematically varied the milling time between 10 min and 90 min

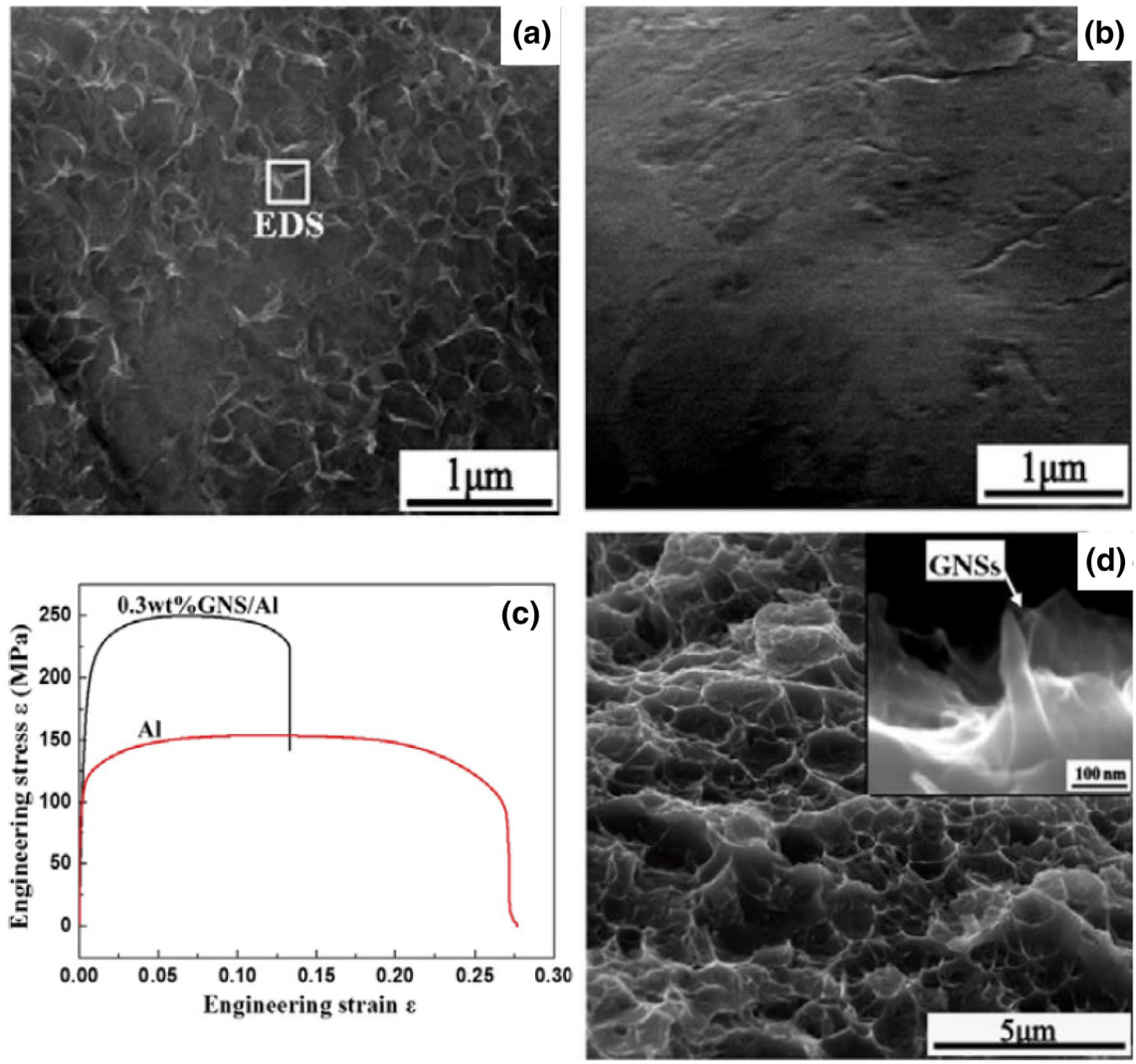

Fig. 3. (a) SEM image of an aluminum flake surface with adsorbed graphene nanosheets. (b) SEM image of an aluminum flake surface without graphene nanosheets. (c) Tensile testing response of 0.3 wt.% GNS/Al composite and the corresponding flake Al specimen. (d) Fracture surface of the 0.3 wt.% GNS/Al composite; the inset shows the GNSs was pulled out[30]

with 1 wt.% graphene in the MMNCs. Monolithic Al6061 samples were also prepared under similar milling times for comparison. A three-point flexural test was performed to compare the mechanical properties of the fabricated samples.

Figure 4 plots the calculated flexural stress–strain responses of both the alloy and MMNC samples based on the milling times. From these responses, it is clear that (1) increasing the milling time increased the strength of both the samples and (2) milling time is critical to achieving improved mechanical properties in the MMNCs with respect to the pure alloys. Considering the individual samples, the increase in flexural strength with a reduction in flexural strain in the pure alloy is attributed to the strain hardening due to milling, while a combination of strain hardening and dispersion of the graphene in the MMNC is attributed to the improved mechanical properties. A comparison of 10-min and 30-min ball-milled samples confirmed that the mechanical properties of the MMNCs did not improve over the pure alloys. This is rationalized by the agglomeration of graphene observed in SEM images in the MMNCs at short milling times. Due to the lack of time, the graphene agglomerates interrupt the consolidation process and generate defects in the composite. By applying bending load, cracks nucleate and grow around the poorly bonded interfacial regions of the agglomerated graphene and matrix phases (Fig. 5), resulting in inferior mechanical properties.

A significant increase (47% and 34%) in flexural strength is reported for the MMNCs over the corresponding pure alloys for 60-min and 90-min milling time, respectively. The longer milling time enables a better distribution of the graphene phase in the matrix with improved interfacial interaction between the two phases. The distributed graphene effectively transfers the load and acts as a barrier to the crack propagation during loading. Therefore, mechanical properties of the MMNCs improve several fold with longer milling times. As the strength of the MMNCs increases from 10 min to 90 min, the fracture morphology changes from ductile to brittle. This is supported by a sharp decrease in the dimple sizes with the presence of numerous flat regions in longer milled samples as observed in SEM analysis.

It is necessary to point out that increasing the milling time does not continuously improve the mechanical properties. This is because of the limited amount of graphene present in the system. Once the graphene reaches a uniform distribution, the milling time has very little effect. This observation is supported by the similar morphologies obtained for 90-min and 300-min milled Gr-Al NCs by Bastwros et al.[26] A similar impact of milling time on hardness variation is reported by Pérez-Bustamante et al.[35] These results highlight the impact of processing parameters on the mechanical properties of Gr-Al NCs.

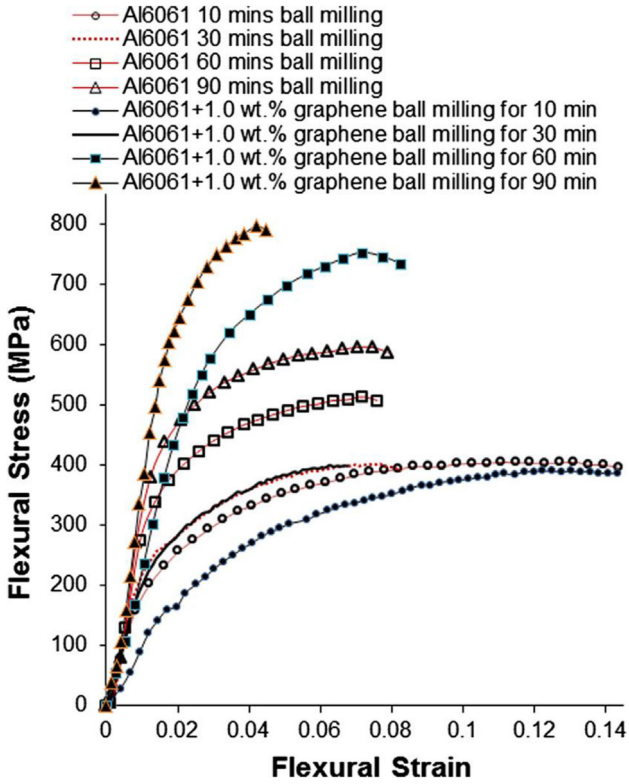

Fig. 4. Flexural stress–strain curves of Al6061-1.0 wt.% graphene composite[26].

The mechanical properties of NCs are observed to improve with increasing graphene content till a particular concentration. A further increase in the graphene content decreases the mechanical properties because of the increased agglomeration.[37] To examine the improvement in the distribution of graphene, Li et al.[23] attempted to simplify the synthesis method discussed in Wang et al.[30] by avoiding the complex step of Al flake surface modification by PVA. Exploiting the electrostatic interaction between GO and Al flakes, Li et al.[23] achieved a better reduction of GO to graphene. The modulus and hardness of Gr-Al NCs with 0.3 wt.% reduced GO were measured to be ~ 18% and 17% higher than unreinforced Al fabricated under similar conditions. Recent research activities focusing on improving the distribution of graphene in Gr-Al NCs to improve the mechanical properties focused on other synthesis parameters such as surface modification of either the matrix or reinforcement[41] and different mixing strategies.[15]

Recent studies on Gr-Al NCs have attempted to use novel techniques or develop cheaper alternatives to the existing synthesis methods. For example, Tabandeh-Khorshid et al.[5] replaced the cryomilling under liquid nitrogen and steric acid followed by high-temperature/vacuum drying steps with less expensive room-temperature milling in ethanol with low-temperature atmospheric drying

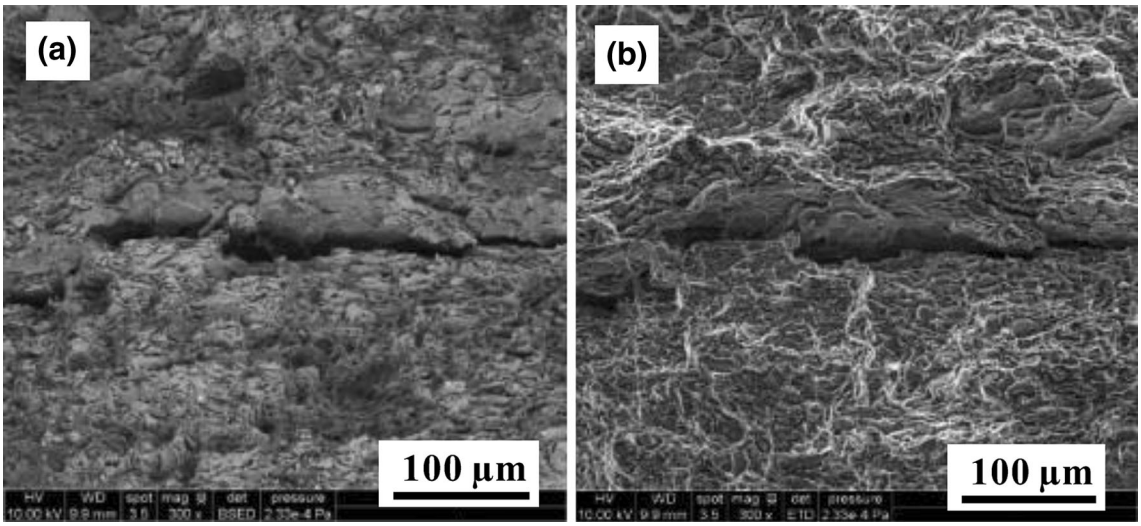

Fig. 5. SEM images of the fracture surface of Al6061-1.0 wt.% graphene composite milled for 10 min showing a large crack that appeared on the surface: (a) BSEC detector and (b) ETD detector[26].

using the PM route. In addition to strength and hardness, variation in tribologic properties of Gr-Al NCs regarding the amount of graphene nanoplatelets (GNPs) is reported. A small quantity of GNPs (0.1 wt.%) in the Al matrix did not affect the coefficient of friction, while larger amounts (1 wt.%) reduced the coefficient of friction because of the formation of graphene film on the worn surface that led to self-lubricating characteristics.[4]

APPLICATIONS

The superior properties of MMNCs are ideal for many engineering applications, including the aviation, electronic packaging, high-end sports equipment and automotive industries. With the accelerated development of novel synthesis technologies for Gr-Al NCs, replacing conventional structural materials such as steel or cast irons components is a growing possibility. Available literature has analyzed the properties of graphene-reinforced nanocomposite for applications in automobiles.[50] Some of these load-bearing and structural parts may be made from Gr-Al NCs, which are designed to provide strength, thermal stability and improved tribologic characteristics over conventional alloys. Engine cylinder liners made of reinforced Al MMCs can improve engine-operating efficiency by reducing knocking because of improved heat transfer from the cylinder to the water jacket.[50,51] Additionally, MMCs with high strength, a low coefficient of thermal expansion and low thermal conductivity can be inserted at the piston combustion face for reducing diesel engines emissions by operating at higher temperatures.[50,51] Overall, efficient manufacturing of graphene-based MMNCs with tunable mechanical, electrical, thermal properties and functionality will expand the engineering application of these unique materials.

SUMMARY AND FUTURE PERSPECTIVE

Graphene-reinforced Al composites have seen increased interest in the last decade. The high specific strength, low density and high corrosion resistance of the Al matrix and extremely high strength, high modulus, and superior electrical, thermal and optical properties of graphene are combined to tailor a wide range of properties in the MMNCs. Theoretical predictions based on uniform distribution of aligned single-layer defect-free graphene sheets in the Al matrix show the potential to develop composites with exceptional properties. However, practical considerations such as agglomeration of graphene, folding and misalignment, and defects lead to properties much lower than those theoretically calculated. Based on these observations, there is a tremendous potential for high-impact contributions to improving the properties of Gr-Al NCs. Optimization of process parameters in synthesis methods, development of novel synthesis techniques, and improving the quality and dispersion of graphene are some of the potential areas of research that can benefit this field. Computational investigations at the level of density functional theory (DFT) and molecular dynamics (MD) are ideal tools to examine the fundamental mechanisms at the nanometer scale such as the Gr-Al interfacial properties, folding or agglomeration of graphene sheets in the Al matrix, properties of single layer vs. multilayer graphene sheets, impact of defects in graphene, and effect of temperature and pressure on consolidation. Hence, it is expected that the

computational studies[24,52] will positively complement the experimental efforts and assist in accelerating the progress in Gr-Al NCs.

ACKNOWLEDGEMENTS

Support from the US National Science Foundation Grant IIA-445686 is acknowledged. The views presented in this article are those of authors, not of the funding agency.

REFERENCES

1. *ASM Handbook Volume 02 - Properties and Selection: Nonferrous Alloys and Special-Purpose Materials* (Russell: ASM International, 1990).
2. D.B. Miracle, *Compos. Sci. Technol* 65, 2526 (2005).
3. A. Dorri Moghadam, E. Omrani, P.L. Menezes, and P.K. Rohatgi, *Compos. B Eng.* 77, 402 (2015).
4. M. Tabandeh-Khorshid, E. Omrani, P.L. Menezes, and P.K. Rohatgi, *Eng. Sci. Technol. Int. J.* 19, 463 (2016).
5. M. Tabandeh-Khorshid, J.B. Ferguson, B.F. Schultz, C.-S. Kim, K. Cho, and P.K. Rohatgi, *Mater. Des.* 92, 79 (2016).
6. Y. Zhu, S. Murali, W. Cai, X. Li, J.W. Suk, J.R. Potts, and R.S. Ruoff, *Adv. Mater.* 22, 3906 (2010).
7. A. Nieto, A. Bisht, D. Lahiri, C. Zhang, and A. Agarwal, *Int. Mater. Rev.* 62, 241 (2017).
8. A.C. Ferrari, F. Bonaccorso, V. Fal'Ko, K.S. Novoselov, S. Roche, P. Bøggild, S. Borini, F.H. Koppens, V. Palermo, and N. Pugno, *Nanoscale* 7, 4598 (2015).
9. K. Novoselov, A.K. Geim, S. Morozov, D. Jiang, M. Katsnelson, I. Grigorieva, S. Dubonos, and A. Firsov, *Nature* 438, 197 (2005).
10. D. Abergel, V. Apalkov, J. Berashevich, K. Ziegler, and T. Chakraborty, *Adv. Phys.* 59, 261 (2010).
11. A. Geim, *Phys. Scr.* 2012, 014003 (2012).
12. H.C. Schniepp, J.-L. Li, M.J. McAllister, H. Sai, M. Herrera-Alonso, D.H. Adamson, R.K. Prud'homme, R. Car, D.A. Saville, and I.A. Aksay, *J. Phys. Chem. B* 110, 8535 (2006).
13. D. Arco, L. Gomez, Y. Zhang, A. Kumar, and C. Zhou, *IEEE Trans. Nanotechnol.* 8, 135 (2009).
14. T. Zhou, F. Chen, K. Liu, H. Deng, Q. Zhang, J. Feng, and Q. Fu, *Nanotechnology* 22, 045704 (2010).
15. H. Asgharzadeh and M. Sedigh, *J. Alloy. Compd.* 728, 47 (2017).
16. S.-J. Yan, C. Yang, Q.-H. Hong, J.-Z. Chen, D.-B. Liu, and S.-L. Dai, *J. Mater. Eng.* 1, 1 (2011).
17. K. Novoselov and A.C. Neto, *Phys. Scr.* 2012, 014006 (2012).
18. W. Ren and H.-M. Cheng, *Nat. Nanotechnol.* 9, 726 (2014).
19. A. Reina, X. Jia, J. Ho, D. Nezich, H. Son, V. Bulovic, M.S. Dresselhaus, and J. Kong, *Nano Lett.* 9, 30 (2009).
20. D. Barun, K.E. Prasad, U. Ramamurty, and C.N.R. Rao, *Nanotechnology* 20, 125705 (2009).
21. T. Kuilla, S. Bhadra, D. Yao, N.H. Kim, S. Bose, and J.H. Lee, *Prog. Polym. Sci.* 35, 1350 (2010).
22. G. Mittal, V. Dhand, K.Y. Rhee, S.-J. Park, and W.R. Lee, *J. Ind. Eng. Chem.* 21, 11 (2015).
23. Z. Li, G. Fan, Z. Tan, Q. Guo, D. Xiong, Y. Su, Z. Li, and D. Zhang, *Nanotechnology* 25, 325601 (2014).
24. Z. Xu and M.J. Buehler, *J. Phys. Condens. Matter* 22, 485301 (2010).
25. F.H. Latief, E.-S.M. Sherif, A.A. Almajid, and H. Junaedi, *J. Anal. Appl. Pyrol.* 92, 485 (2011).
26. M. Bastwros, G.-Y. Kim, C. Zhu, K. Zhang, S. Wang, X. Tang, and X. Wang, *Compos. B Eng.* 60, 111 (2014).
27. H. Zhang, C. Xu, W. Xiao, K. Ameyama, and C. Ma, *Mater. Sci. Eng., A* 658, 8 (2016).
28. S.J. Yan, S.L. Dai, X.Y. Zhang, C. Yang, Q.H. Hong, J.Z. Chen, and Z.M. Lin, *Mater. Sci. Eng., A* 612, 440 (2014).
29. W. Yang, G. Chen, J. Qiao, S. Liu, R. Xiao, R. Dong, M. Hussain, and G. Wu, *Mater. Sci. Eng., A* 700, 351 (2017).
30. J. Wang, Z. Li, G. Fan, H. Pan, Z. Chen, and D. Zhang, *Scr. Mater.* 66, 594 (2012).
31. S.F. Bartolucci, J. Paras, M.A. Rafiee, J. Rafiee, S. Lee, D. Kapoor, and N. Koratkar, *Mater. Sci. Eng. A* 528, 7933 (2011).
32. F.H. Latief and E.-S.M. Sherif, *J. Ind. Eng. Chem.* 18, 2129 (2012).
33. A. Ghazaly, B. Seif, and H.G. Salem, *Light Metals 2013* (Hoboken: Wiley, 2013), p. 411.
34. C.-H. Jeon, Y.-H. Jeong, J.-J. Seo, H.N. Tien, S.-T. Hong, Y.-J. Yum, S.-H. Hur, and K.-J. Lee, *Int. J. Precis. Eng. Manuf.* 15, 1235 (2014).
35. R. Pérez-Bustamante, D. Bolaños-Morales, J. Bonilla-Martínez, I. Estrada-Guel, and R. Martínez-Sánchez, *J. Alloy. Compd.* 615, S578 (2014).
36. M. Rashad, F. Pan, A. Tang, and M. Asif, *Prog. Nat. Sci. Mater. Int.* 24, 101 (2014).
37. J.L. Li, Y.C. Xiong, X.D. Wang, S.J. Yan, C. Yang, W.W. He, J.Z. Chen, S.Q. Wang, X.Y. Zhang, and S.L. Dai, *Mater. Sci. Eng. A* 626, 400 (2015).
38. S.E. Shin, H.J. Choi, J.H. Shin, and D.H. Bae, *Carbon* 82, 143 (2015).
39. S.E. Shin, Y.J. Ko, and D.H. Bae, *Compos. B Eng.* 106, 66 (2016).
40. K.H.G Prashantha and X.M. Anthony, in *Graphene Materials - Structure, Properties and Modifications*, ed. by G.Z. Kyzas, A. C. Mitropoulos (InTech, Rijeka, 2017), pp. Ch. 07.
41. G. Liu, N. Zhao, C. Shi, E. Liu, F. He, L. Ma, Q. Li, J. Li, and C. He, *Mater. Sci. Eng. A* 699, 185 (2017).
42. J. Wozniak, M. Kostecki, T. Cygan, M. Buczek, and A. Olszyna, *Compos. B Eng.* 111, 1 (2017).
43. C. Tomasz, E.A. Korznikova, P. Ozga, L.Lityńska, and R.P. Socha, Innovative Manufacturing Technology IMT 2014, Krakow, Poland (2014).
44. L. Ci, Z. Ryu, N.Y. Jin-Phillipp, and M. Rühle, *Acta Mater.* 54, 5367 (2006).
45. M.A. Rafiee, J. Rafiee, I. Srivastava, Z. Wang, H. Song, Z.Z. Yu, and N. Koratkar, *Small* 6, 179 (2010).
46. M.A. Rafiee, J. Rafiee, Z. Wang, H. Song, Z.-Z. Yu, and N. Koratkar, *ACS Nano* 3, 3884 (2009).
47. L. Jiang, Z. Li, G. Fan, L. Cao, and D. Zhang, *Carbon* 50, 1993 (2012).
48. C. Lee, X. Wei, J.W. Kysar, and J. Hone, *Science* 321, 385 (2008).
49. S. Wang, M. Tambraparni, J. Qiu, J. Tipton, and D. Dean, *Macromolecules* 42, 5251 (2009).
50. A. Elmarakbi, W.L. Azoti, in 10th *International Conference on Composite Science and Technology Lisboa, Portugal*, September 2–4, 2015 (2015).
51. G.S. Cole and A.M. Sherman, *Mater. Charact.* 35, 3 (1995).
52. A. Ilyin, G. Beall, in *Proceedings of the Nanotech*, June 13–16, Boston, USA, vol. 1, Ch. 5, p. 574–576 (2011).